別紙4

研究成果の刊行に関する一覧表レイアウト

書籍

著者氏名	論文タイトル名	書籍全体の編集者名	書籍名	出版社名	出版地	出版年	ページ
1) Nakamura H, et al.	Hepatocellular carcinoma: Prognosis using hepatoma-derived growth factor immunohistochemistry	Hayat M.A.	Methods of Cancer Diagnosis, Therapy and Prognosis	ELSEVIER Academic Press	USA	2009	333-342

雑誌

発表者氏名	論文タイトル名	発表誌名	巻号	ページ	出版年
1) Xu X,et al.	CDC25A inhibition suppresses the growth and invasion of human hepatocellular carcinoma cells	Int J Mol Med	21(2)	145-152	2008
2) Kittaka N,et al.	Molecular mapping of human hepatocellular carcinoma provides deeper biological insight from genomic data	Eur J Cancer	44	885-897	2008
3) Eguchi S,et al.	Comparison of the outcomes between an anatomical subsegmentectomy and a non-anatomical minor hepatectomy for single hepatocellular carcinomas based on a Japanese nationwide survey	Surgery	143(4)	469-475	2008
4) Uyama H,et al.	New chemotherapy for patients with advanced hepatocellular carcinoma: Pilot study of -interferon and doxorubicin one-shot intra-arterial chemotherapy	Hepatology Research	37(12)	1018-102	2007
5) Hasegawa K,et al.	Surgical resection vs. percutaneous ablation for hepatocellular carcinoma: A preliminary report of the Japanese nationwide survey	Journal of Hepatology	49(4)	589-594	2008
6) Nakamura M, et al.	Pilot study of combination chemotherapy of S-1, a novel oral DPD inhibitor, and interferon-α for advanced hepatocellular carcinoma with extrahepatic metastasis	Cancer	112(8)	1766-177	2008
7) 野田剛広, 他	消化器がんの化学療法-外科の立場から肝がん	Medico	39(1)	10-14	2008
8) 村上昌裕, 他	Doxorubicin/IFN-β併用化学療法と肝切除術により長期生存し得た右心房内腫瘍栓を伴う進行肝細胞癌の1例	癌と化学療法	34(12)	2087-208	2008
9) 永野浩昭, 他	5FUとインターフェロン	肝胆膵	55(5)	823-831	2007
10) 小林省吾, 他	治療の進歩と問題点 治療後再発予防に関する知見	外科治療	98(2)	174-177	2008
11) 門田守人	肝癌に対するインターフェロン併用化学療法の基礎と臨床	肝臓病学の進歩	29	39-44	2008
12) 永野浩昭, 他	肝細胞癌の集学的治療と化学療法	外科	70(2)	192-196	2008

13) 永野浩昭, 他	術前・術後の補助療法	消化器外科	31(6)	999-1006	2008
14) 浅岡忠史, 他	肝細胞癌合併非代償性肝硬変に対する肝転移直後の肺転移再発5例の治療経験	癌と局所療法	35(12)	2086-208	2008
15) 野田剛広, 他	IFN-α/5-FU併用動注化学療法治療後に無効病巣の出現および他臓器浸潤に対して切除術を施行した混合型肝癌の1例	癌と化学療法	35(12)	2099-210	2008
16) 武田裕, 他	原発性肝癌に対するadjuvant/neoadjuvant chemotherapy	臨床外科	63(13)	1715-172	2008
17) 野田剛広, 他	補助化学療法の適応は？	消化器癌の外科治療		51-56	2008
18) Kanda M et al.	Extrahepatic metastasis of hepatocellular carcinoma: incidence and risk factors.	Liver Int.	28(9)	1256-1263	2008
19) Imamura J et al.	Neoplastic seeding after radiofrequency ablation for hepatocellular carcinoma.	Am J Gastroenterol.	103(12)	3057-3062	2008
20) Tateishi R et al.	Treatment strategy for hepatocellular carcinoma: expanding the indications for radiofrequency ablation.	J Gastroenterol.	44 Suppl 19	142-146	2009
21) 小尾俊太郎	【腫瘍栓のすべて】切除以外の治療 インターフェロンの併用動注療法(2)	外科	70 (2)	197-202	2008
22) Oishi K, et al	Hepatectomy for Hepatocellular Carcinoma in Elderly Patients Aged 75 Years or More.	J Gastrointest Surg.			2008
23) Luo KZ,et al	Comparative study of the Japan Integrated Stage (JIS) and modified JIS score as a predictor of survival after hepatectomy for hepatocellular carcinoma.	J Gastroenterol.	43(5)	369-377	2008
24) Mizuguchi T, et al.	Rapid recovery of postoperative liver function after major hepatectomy using saline-linked electric cautery.	Hepatogastroenterology	55(88)	2188-219	2008
25) Mizuguchi T, et al.	Prognostic impact of surgical complications and preoperative serum hepatocyte growth factor in hepatocellular carcinoma patients after initial hepatectomy.	J Gastrointest Surg.	13(2)	325-333	2009
26) 久保正二, 他	特集「局所再発癌に対する外科治療;適応とコツ」大血内進展を伴う進行再発肝細胞癌に対する外科治療	消化器外科	31(2)	157-164	2008
27) 久保正二, 他	臨床病理カンファレンス1.B型肝炎と肝細胞癌	綜合臨床	57(6)	1841-185	2008
28) 久保正二, 他	特集 II 再発肝癌診療におけるコンセンサスと個別化:予後因子からみたC型肝炎関連肝細胞癌切除後再発例に対する再肝切除の適応	消化器科	47(1)	85-90	2008
29) 久保正二, 他	特集 どこまで切除するか—良・悪性境界型腫瘍性病変—4. 肝腫瘍	Surgery Frontier	15(3)	33-39	2008
30) 市川 剛, 他	肝切除後肝不全予測における血清中Type IV collagen 7s domainの意義	消化器科	47(5)	585-591	2008
31) 松田常美, 他	肝切除術における腹腔ドレーン抜去時期に関する検討	日本消化器外科学会雑誌	42(2)	142-146	2008

32) 久保正二, 他	C型肝炎由来肝癌治療後の再発予防について	外科	in press		2008
33) 上西崇弘, 他	インターフェロン療法によるC型肝炎関連肝細胞癌の切除成績向上	消化器科	in press		2008
34) Kubo S, et al.	Second hepatic resection for recurennt hepatocellular carcinoma in patients with chronic hepatitis C	World Journal of Surgery	32(4)	632-638	2008
35) Tanaka H, et al.	Convenience of a tape-guiding technique in different types of hepatectomy.	Hepatogastroenterology	55(81)	160-163	2008
36) Uenishi T, et al.	Response to interferon therapy affects risk factors for postoperative recurrence of hepatitis C virus-related hepatocellular	Journal of Surgrical Oncology	98(5)	358-362	2008
37) Shinkawa H,et al.	Hepatocellular carcinoma (HCC) recurring 10 years after clearance of hepatitis B surface antigen and 20 years after resection of hepatitis B virus-related HCC.	International Journal of Clinical Oncology	13(6)	562-566	2008
38) Ichikawa T,et al.	A simple, noninvasively determined index predicting hepatic failure following liver resection for hepatocellular carcinoma	Journal of Hepato-Biliary-Pancreatic Surgery	16(1)	42-48	2009
39) Hayashi T, et al.	Differences in molecular alterations of hepatocellular carcinoma between patients with a sustained virological response and those with hepatitis C virus infection.	Liver International	29(1)	26-32	2009
40) Nakamura H, et al.	Impact of hepatoma-derived growth factor on hepatocellular carcinoma	Current Research in Hepatology	2	45-56	2008
41) Nakamura H, et al.	Involvement of hepatoma-derived growth factor in the growth inhibition of hepatocellular carcinoma cells by vitamin K2	Journal of Gastroenterology	44(3)	228-235	2009
42) Nakamura H, et al.	A higher expression of hepatoma-derived growth factor in hepatocellular carcinoma cells and more tumor growth in vivo	Trends in Cancer Research	in press		2009
43) 中村秀次, 他	胎生期未分化肝細胞の増殖におけるHDGF (Hepatoma-derived growth factor)の役割	消化器疾患におけるTranslational Research		229-230	2008
44) 辻晃仁	外来がん化学療法とチーム医療	外科治療	98	508-515	2008
45) 秦康博, 他	がん化学療法を安全・確実に行うためのレジメンの読み方・見方 レジメンを理解するための基礎知識・用語の解説	がん患者ケア	2(1)	56-63	2008
46) 辻晃仁,他	がん化学療法を安全・確実に行うための レジメンの読み方・見方 大腸がん	がん患者ケア	2(2)	102-119	2008
47) 小林和真,他	がん化学療法を安全・確実に行うためのレジメンの読み方・見方 胃がん	がん患者ケア	2(3)	87-100	2009
48) 西村公男, 他	肝転移巣が下大静脈腫瘍栓を形成した膵ガストリノーマの1例	胆と膵	30(1)	103-107	2009
49) Tsuji A, et al.	Combination Chemotherapy of S-1 and Low-dose Twice-Weekly cisplatin for Advanced and Recurrent Gastric Cancer in an Outpatient Setting: A Retrospective Study	ANTICANCER RESEARCH	28(2B)	1433-1438	2008

CDC25A inhibition suppresses the growth and invasion of human hepatocellular carcinoma cells

XUNDI XU[1,2], HIROFUMI YAMAMOTO[1], GUOXING LIU[2], YASUHIRO ITO[1], CHEW YEE NGAN[1], MOTOI KONDO[1], HIROAKI NAGANO[1], KEIZO DONO[1], MITSUGU SEKIMOTO[1] and MORITO MONDEN[1]

[1]Department of Surgery, Gastroenterological Surgery, Graduate School of Medicine, Osaka University, Osaka 565-0871, Japan; [2]Department of Surgery, Xiangya Second Hospital, Central South University, Changsha, Hunan province 410011, P.R. China

Received May 31, 2007; Accepted July 9, 2007

Abstract. CDC25A is a cell cycle-activating phosphatase that promotes transition from the G1 to S phase. We previously reported that overexpression of CDC25A in human hepatocellular carcinoma (HCC) tissue samples was associated with poor prognosis. In this study, we attempted suppression of CDC25A in HCC cells to elucidate the therapeutic potential of this approach. Administration of CDC25A antisense (AS) oligonucleotide resulted in 25-50% inhibition of cell growth at 48 h, G0-G1 arrest, and significant inhibition of cancer cell invasion. To elucidate the underlying mechanism of the inhibitory effects of HCC cell invasion, we examined several invasion-associated molecules, and we found that membrane-type 3 (MT3)-matrix metalloproteinase (MMP) mRNA was greatly reduced following treatment with AS oligonucleotide to CDC25A or siRNA treatment. Notably, screening of a panel of gastrointestinal cancer cells indicated that MT3-MMP was generally expressed by HCC cells, whereas other cell types did not express this type of matrix metalloproteinase so frequently. We also found that CDC25A facilitated cellular differentiation by increasing albumin expression in the PLC cell line. These results suggest that CDC25A, by inhibiting HCC growth and invasion, may be a feasible therapeutic target for human HCC.

Correspondence to: Dr Hirofumi Yamamoto, Department of Surgery, Gastroenterological Surgery, Graduate School of Medicine, Osaka University, 2-2 Yamada-oka, Suita-City, Osaka 565-0871, Japan
E-mail: kobunyam@surg2.med.osaka-u.ac.jp

Abbreviations: AS, antisense; CDK, cyclin-dependent kinase; dsRNAs, double-stranded RNAs; HCC, hepatocellular carcinoma; MMP, matrix metalloproteinase; MM, mismatch; PBGD, porphobilinogen deaminase; PCNA, proliferating cell nuclear antigen; RT-PCR, reverse transcriptase-polymerase chain reaction; siRNA, short interfering RNA

Key words: CDC25A, membrane-type 3-matrix metalloproteinase, hepatocellular carcinoma, invasion, differentiation

Introduction

Primary hepatocellular carcinoma (HCC) is the third leading cause of cancer death worldwide, with an estimated 564,000 new cases in 2000 (1). Frequent postoperative recurrence of the disease, characterized by intrahepatic metastasis or multicentric carcinogenesis, is one of the major reasons for the poor prognosis of HCC (2,3). Insight into the molecular mechanisms involved in hepatocarcinogenesis may enable more effective treatment for HCC.

CDC25 genes are cell cycle-activating phosphatases that remove the inhibitory phosphates of threonine and tyrosine residues at the ATP-binding sites of cyclin-dependent kinase. Three CDC25 genes, CDC25A, CDC25B, and CDC25C, which share ~40-50% amino acid identity, have been identified and function during different stages of the cell cycle, including G1-S and G2-M transition (4-7). It has been found that CDC25A and CDC25B, but not CDC25C, possess oncogenic potential and are able to transform primary murine fibroblasts in cooperation with either mutated Ha-ras or loss of Rb1 (8). Furthermore, concordant *in vitro* and *in vivo* findings show that CDC25A and CDC25B are overexpressed in various types of human malignancies, including HCC (9-14).

Accumulating evidence suggests that several molecules acting at the G1-S transition of the cell cycle play crucial roles in the progression of HCC. HCC tissues overexpress cyclins D1 and E (15,16). In a subset of HCCs, expression of the cyclin-dependent kinase (CDK) inhibitor $p21^{waf1/cip1}$ was reduced, the $p16^{INK4}$ gene was methylated at the promoter region, and expression of $p27^{Kip1}$ appeared to be decreased (15,17,18). We previously found that CDC25A, rather than CDC25B, was overexpressed in the dedifferentiated phenotype of HCC and that its levels correlated with hypergrowth activity (14). We also found that CDC25A overexpression was associated with shorter disease-free survival of patients with HCC. Foundational research showed that ablation of CDC25A function by microinjection of a specific antibody blocks cell entry into S phase (5). Conversely, inducible overexpression of CDC25A, leading to activation of cyclin E-Cdk2 and cyclin A-Cdk2, revealed that these complexes act as critical targets for CDC25A (19,20). This evidence suggests the relevance of CDC25A to G1-S transition. Based

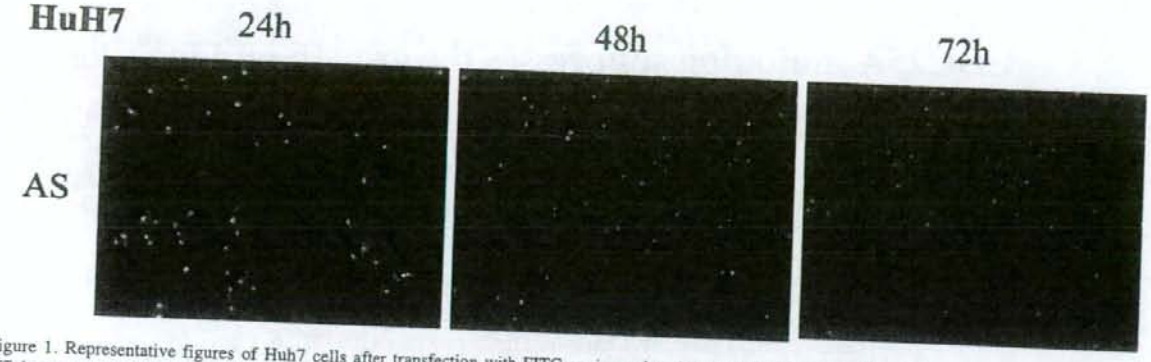

Figure 1. Representative figures of Huh7 cells after transfection with FITC-conjugated antisense (AS) oligonucleotides. Cell count indicated transfection efficiency at 84.1, 88.0 and 89.7% at 24, 48 and 72 h, respectively.

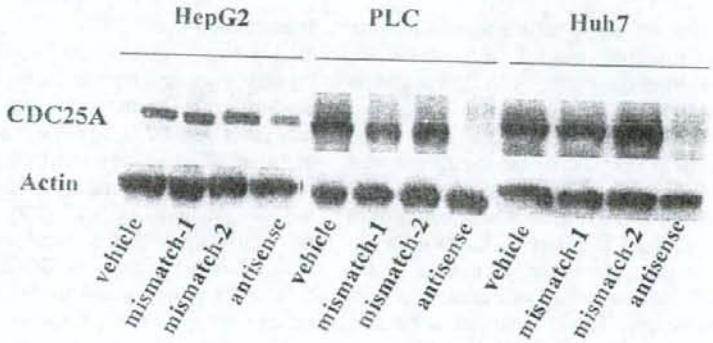

Figure 2. AS oligonucleotide to CDC25A decreased CDC25A expression in HCC cells. Three HCC cell lines were transfected with vehicle alone, vehicle plus MM oligonucleotides, or AS oligonucleotides. Cells were harvested 48 h after transfection. The protein lysates were subjected to Western blot analysis with anti-CDC25A and anti-actin antibody. Actin bands indicate equal loading of the protein.

MT2-MMP reverse, 5'-CTT TCA CTC GTA CCC CGA AC-3'; MT3-MMP forward, 5'-ACA GTC TGC GGA ACG GAG CAG-3' and MT3-MMP reverse, 5'-GTC AAT TGT GTT TCT GTC CAC-3'.

Statistical analysis. Data were expressed as the mean ± SEM. Group differences were examined for statistical significance using the Mann-Whitney U test or Fisher's exact test. Mean values were compared using the Student's t-test. A $p<0.05$ denoted a statistically significant difference.

Results

Transfection efficiency. Representative figures of cells transfected with FITC-conjugated oligonucleotides are shown in Fig. 1. PLC cells had a lowest transfection efficiency, with an average of 18.8±4.57 and 19.5±5.76% for AS and MM2, respectively. A tendency of reduction of efficiency with time was noted. A lower efficiency was found for MM1 at 13.2±0.23%. A slightly higher efficiency was noted in HepG2; 29.6±4.20% for AS, 30.3±1.08% for MM2 and similarly a lower rate of 21.9±7.47% for MM1. Reduction of efficiency with time was only observed for MM1. The highest transfection efficiency was observed for Huh7; 87.2±2.79%, 87.5±1.23% and 86.7±5.48 for AS, MM1 and MM2 respectively.

Suppression of CDC25A with antisense oligonucleotides. We used Western blotting to examine the expression of CDC25A protein in HepG2, PLC, and Huh7 HCC cell lines treated with vehicle alone or vehicle plus each oligonucleotide (AS, MM-1, or MM-2) 48 h after transfection. As shown in Fig. 2, the AS oligonucleotide suppressed CDC25A levels by 60% in HepG2 cells and by ~95% in PLC and Huh7 cells. On the other hand, when we examined CDC25B expression no reduction was obtained by AS-CDC25A (data not shown).

Cell growth and cell cycle. AS to CDC25A significantly inhibited cell growth of HepG2, PLC, and Huh7 cells. Statistical significance between cultures treated with AS oligonucleotide versus other oligonucleotides is shown in Fig. 3A. We then performed flow cytometric analysis 24 h after transfection. In the three HCC cell types tested, treatment with AS oligonucleotide increased the G0-G1 phase fraction and decreased the S phase fraction when compared to vehicle-treated cultures. Repeat experiments of cell growth and cell cycle analyses gave similar results. A representative result is shown in Fig. 3B with the following fraction values for

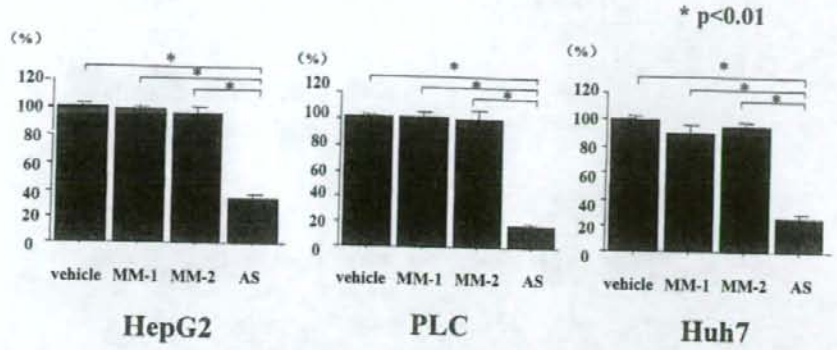

Figure 4. Invasion assay. AS to CDC25A decreased invasion by HCC cells. The assay was performed in duplicate; bars indicate the mean ± SD. A significant reduction in cell invasion was noted in AS-treated cultures versus cultures treated with vehicle, MM-1, and MM-2 (*p<0.01).

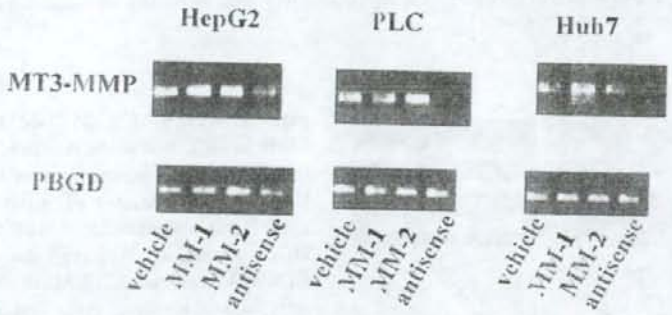

Figure 5. AS to CDC25A decreased MT3-MMP mRNA expression in HCC cells. Cells were harvested 24 h after transfection and examined for MT3-MMP mRNA by RT-PCR assay. PBGD, a housekeeping gene, served as the control. HCC tissues were used as positive control for MT3-MMP mRNA.

Invasive ability. To investigate the effect of AS to CDC25A on the invasive ability of HCC cells we performed an invasive assay. When compared to vehicle treatment, AS to CDC25A significantly suppressed cancer cell invasion by 33.2% in HepG2 cells (p=0.002), 17.2% in PLC cells (p=0.001), and 26.5% in Huh7 cells (p=0.001) (Fig. 4). These inhibitory effects were not found with MM-1 or MM-2 treatment. A repeat experiment showed similar results.

Expression of matrix metalloproteinases. To investigate the underlying mechanism for the inhibitory effect of AS to CDC25A on the invasive ability of HCC cells, we used RT-PCR to examine the expression of a series of matrix metalloproteinases (MMP). These included MMP2, MT1-MMP, MT2-MMP, and MT3-MMP. We found that AS to CDC25A decreased MT3-MMP mRNA expression in all three HCC cell lines (Fig. 5). However, expression of the other MMPs was unaffected (data not shown). To confirm the results, we investigated the effect of siRNA against CDC25A. Western blot analysis showed that the reduction in CDC25A expression was associated with a large reduction in MT3-MMP protein in the three HCC cell lines (Fig. 6).

We then investigated mRNA expression of MMP2, MT1-MMP, MT2-MMP, and MT3-MMP in a variety of gastrointestinal tumor cell lines including HCC cell lines. MT3-MMP expression, when compared to that of other MMPs, was relatively specific to the HCC cell lines (expression rate by cell lines, 7/7:100%) versus other gastrointestinal tumor cell lines such as pancreatic cancer (2/5:40%), colon cancer (0/5: 0%), gastric cancer (1/5:20%), and esophageal cancer (1/3:33%) cell lines (Table 1).

Restoration of albumin expression in PLC by CDC25A inhibition. We investigated whether inhibition of CDC25A restores cell differentiation in HCC cell lines, using albumin expression as a marker of differentiation (24). We found that the PLC cell line which marginally expressed albumin showed an increase in albumin mRNA expression following treatment with AS oligonucleotide (Fig. 7). siRNA treatment against CDC25A showed a similar result (Fig. 7). However, there was no change in albumin mRNA expression in the remaining two HCC cell lines that had relatively high albumin levels (data not shown). We should also emphasize that this was not the case with other liver-specific functions such as APOCIII or asialoglycoprotein receptor, and glutathione-S-transferase-π (data not shown).

Discussion

In our earlier study of CDC25A expression in human HCC tissue samples we found that high CDC25A expression was associated with cell proliferation, portal vein invasion, and

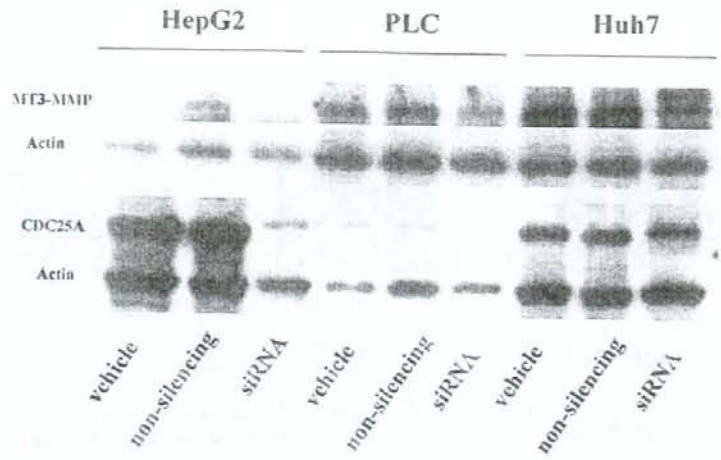

Figure 6. MT3-MMP protein expression was suppressed by siRNA against CDC25A. Cells were collected 48 h after transfection. Inhibition of CDC25A expression by siRNA caused downregulation of MT3-MMP protein expression in HCC cells. By contrast, a non-silencing sequence did not alter CDC25A or MT3-MMP levels. Actin blots served as a loading control.

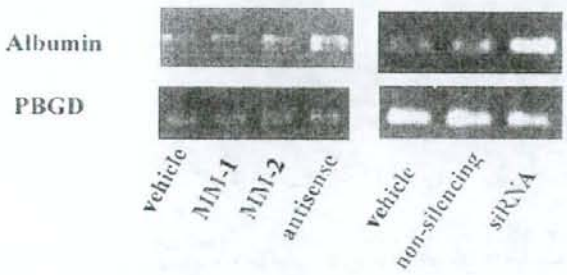

Figure 7. Inhibition of CDC25A induced albumin mRNA expression in PLC cells. AS to CDC25A and siRNA against CDC25A induced expression of albumin mRNA as early as 12 h after treatment. PBGD served as the control.

HCC by restraining growth, which may lead to prolonged disease-free survival.

We also found that AS to CDC25A inhibited the invasive activity of HCC cell lines. This finding is particularly important because HCC invades vessel walls and metastasizes inside the liver, which is considered a major cause of death from the disease (29,30). It may be argued that the inhibitory effects of AS to CDC25A on cancer cell invasion may simply reflect reduced tumor cell growth. We cannot rule out such a possibility. Yet based on the demonstrated downregulation of MT3-MMP in all three HCC cell lines it is likely that the invasive ability itself may be regulated by AS to CDC25A. MT3-MMP, one of the major MMPs, was originally cloned from human melanoma tissue and human placenta and is expressed in a variety of normal and tumor tissues (22,31-33). Functional expression of MT3-MMP in human WM1341D melanoma cells facilitated *in vitro* collagen I invasion (34). Also, expression of MT3-MMP in hamster CHO-K1 and canine MDCK cells induced the expression of a fibrin-invasive phenotype (35). When we examined the mRNA expression of MMP2, MT1-MMP, MT2-MMP, and MT3-MMP in HCC and gastrointestinal cancer cell lines, we found that MT3-MMP expression was rather specific to HCC cell lines. Moreover, we recently found that MT3-MMP expression was associated with tumor invasion in primary HCC tissues (36). Although the precise mechanism of how CDC25A regulates MT3-MMP should be determined at the next stage of research, these findings suggest the relevance of MT3-MMP to invasion in HCC.

Our previous study showed that CDC25A expression was associated with dedifferentiated histology of HCC (14). In the present mechanistic study, we found upregulation of albumin mRNA in PLC cells treated with CDC25A AS. It is reported that PLC produces albumin scarcely, while Huh-7 and HepG2 cells produce high albumin levels (37-39), which is consistent with current findings. The difference in basal albumin level may account for restoration of albumin expression only in PLC cells. Human HCC is unique in that tumor growth occurs relatively slowly and with a well-differentiated phenotype in the early stage but faster and with dedifferentiation in the advanced stage (40,41). In this context, inhibition of CDC25A may convert advanced HCC into a more differentiated and less aggressive phenotype; at least certain types of HCC cells.

In conclusion, antagonism of CDC25A inhibited the growth and invasion of HCC cells, possibly via cell cycle arrest at G0-G1 and suppression of MT3-MMP expression. Taken together, these findings strongly suggest that CDC25A may be a promising therapeutic target against HCC. Indeed, several CDC25A inhibitors are being developed, including novel vitamin K analogues and steroidal-derived inhibitors (42,43).

Acknowledgements

This study was supported by a Grant-in Aid for Cancer Research from the Ministry of Education, Science, Sports, Culture, and Technology, Japan to H.Y.

EUROPEAN JOURNAL OF CANCER 44 (2008) 885–897

available at www.sciencedirect.com

ScienceDirect

journal homepage: www.ejconline.com

Molecular mapping of human hepatocellular carcinoma provides deeper biological insight from genomic data

Nobuyoshi Kittaka[a], *Ichiro Takemasa*[a,*], *Yutaka Takeda*[a], *Shigeru Marubashi*[a], *Hiroaki Nagano*[a], *Koji Umeshita*[a], *Keizo Dono*[a], *Kenichi Matsubara*[b], *Nariaki Matsuura*[c], *Morito Monden*[a]

[a]*Department of Surgery, Graduate School of Medicine, Osaka University, 2-2 Yamadaoka E-2, Suita, Osaka 565-0871, Japan*
[b]*DNA Chip Research Inc., 1-1-43 Suehirocho, Tsurumi-ku, Yokohama 230-0045, Japan*
[c]*Department of Functional Diagnostic Science, Osaka University Graduate School of Medicine, 1-7 Yamadaoka, Suita, Osaka 565-0871, Japan*

ARTICLE INFO

Article history:
Received 5 December 2007
Received in revised form
5 February 2008
Accepted 12 February 2008
Available online 11 March 2008

Keywords:
DNA microarray
Network analysis
Integrative method
'Hotspot' region
Biological insight

ABSTRACT

DNA microarray analysis of human cancer has resulted in considerable accumulation of global gene profiles. However, extraction and understanding the underlying biology of cancer progression remains a significant challenge. This study applied a novel integrative computational and analytical approach to this challenge in human hepatocellular carcinoma (HCC) with the aim of identifying potential molecular markers or novel therapeutic targets. We analysed 100 HCC tissue samples by human 30 K DNA microarray. The gene expression data were uploaded into the network analysis tool, and the biological networks were displayed graphically. We identified several activated 'hotspot' regions harbouring a concentration of upregulated genes. Several 'hotspot' regions revealed integrin and Akt/NF-κB signalling. We identified key members linked to these signalling pathways including osteopontin (SPP1), glypican-3 (GPC3), annexin 2 (ANXA2), S100A10 and vimentin (VIM). Our integrative approach should significantly enhance the power of microarray data in identifying novel potential targets in human cancer.

1. Introduction

Investigation of various cancers at the molecular level is well underway through functional approaches including DNA microarray technology that can simultaneously detect the expression levels of tens of thousands of genes. The resulting wealth of data has been analysed with a variety of clustering, partitioning and pattern-matching algorithms in the quest to generate molecular signatures for several human malignant tumours with respect to their stage, prognostic outcome and response to therapy.

Notwithstanding the obvious power of the genomic data generated, these molecular analyses have not yielded the expected advances in our understanding of the mechanisms of cancer development, or the identification of critical genomic and molecular aberrations that would improve the precision of diagnosis or serve as therapeutic targets. This is mainly due to the overwhelming diversity of genome-wide interactions and gene-expression patterns, which limit effective learning from experimental data alone. Network analysis technologies are currently addressing this problem by mapping the gene expression data into relevant networks based on known mammalian biology, derived from basic and clinical research. To this end, our group has combined microarray analysis with a computational tool to obtain further biological insights into the regulatory networks of differentially expressed genes and

* *Corresponding author*: Tel.: +81 6 6879 3251; fax: +81 6 6879 3259.
E-mail address: alfa-t@sf6.so-net.ne.jp (I. Takemasa).
0959-8049/$ - see front matter © 2008 Elsevier Ltd. All rights reserved.
doi:10.1016/j.ejca.2008.02.019

the corresponding canonical pathways related to the progression of cancer. We applied this integrative approach to human hepatocellular carcinoma (HCC), the fifth most common malignancy worldwide.[1,2] Despite the remarkable improvements in diagnosis and patient management, the outcome for patients with HCC remains grave, mainly due to the advanced tumour stage accelerated by intrahepatic tumour spread and frequent tumour recurrence.[3] Hepatocarcinogenesis is a multistep process involving somatic mutations, loss of tumour suppressor genes and possibly the activation or overexpression of certain oncogenes.[4] These events lead to changes in the expression of numerous genes, and comparison of gene expression patterns between HCC and normal liver tissue is a popular method for characterising tumour properties and identifying novel target genes for possible therapy. However, this method has not proven to be sufficiently definitive in identifying genetic determinants of specific HCC regulatory pathways. New approaches are urgently needed to better understand the underlying mechanisms of hepatocarcinogenesis, and to develop new therapeutic approaches targeted to HCC-specific molecular abnormalities. By highlighting several activated regions in the genome (known as 'hotspot' regions[5,6]) involved in regulating the progression of HCC, we have identified significantly upregulated genes linked to these 'hotspot' pathways as potential key molecules.

Our integrative analysis revealed two 'hotspot' canonical pathways (integrin and Akt/NF-κB signalling pathways) and identified five potential key genes that were upregulated in the majority of HCC tumours. We further investigated two of these potential key molecules, ANXA2 and S100A10, which were upregulated at the protein and mRNA levels in most HCC samples. Importantly, because it is proteins that function in networks controlling critical cellular events,[7] it is reasonable to speculate that coexpression of ANXA2 and S100A10 at the protein level might have an impact on hepatocarcinogenesis through the activated 'hotspot' pathway.

2. Materials and methods

2.1. *Tissue samples*

Samples from 100 HCC tissues and seven normal livers without virus infection were obtained with informed consent from patients who underwent hepatic resection at Osaka University Hospital from 1997 to 2003. Tissue specimens (approximately 5 mm^3) for RNA isolation were stored at −80 °C until use. All tissue specimens were submitted for routine pathological evaluation and confirmation of diagnosis. The histopathological characterisation of HCC was based on the Classification of the Liver Cancer Study Group of Japan. Table 1 lists the clinicopathological features of the 100 cases of HCC.

2.2. *Extraction and quality assessment of RNA*

Total RNA was purified from tissue samples using TRIzol reagent (Invitrogen, San Diego, CA) as described by the manufacturer. The integrity of RNA was assessed on an Agilent 2100 Bioanalyzer and RNA 6000 LabChip kits (Yokokawa Ana-

Table 1 – Clinicopathological characteristics of 100 patients with HCC

Clinicopathological features	*n*
Age	
Median	66
Range	47–81
Gender	
Male	81
Female	19
Virus	
HBV	21
HCV	40
Both	28
None	11
Child-Turcotte-Pugh stage	
A	77
B	23
C	0
Liver cirrhosis	
Present	42
Absent	58
AFP	
<200 ng/ml	71
⩾200 ng/mg	29
PIVKA-II	
<50mAU/ml	36
⩾50mAU/ml	64
Tumour size	
<5.0 cm	76
⩾5.0 cm	24
Edmonson grading	
1–2	43
3–4	57
Histologic type of tumour	
Well differentiated	4
Moderately differentiated	41
Poorly differentiated	55
Vascular invasion	
Present	41
Absent	59
Intrahepatic metastasis	
Present	22
Absent	78
Pathological stage	
I	23
II	52
III	20
IVA	5
CLIP score	
0	56
1	35
2	8
3	0
4	1
5	0
6	0
JIS score	
0	18
1	46
2	26
3	9
4	1
5	0

CLIP score; The cancer of Liver Italian Program score.
JIS score; The Japan Integrated Staging score.

lytical Systems, Tokyo, Japan). Only high-quality RNA with intact 18s and 28s RNA was used for subsequent analysis. Seven RNA extractions from different normal liver tissue were mixed as the control reference.

2.3. *Preparation of fluorescently labelled aRNA targets and hybridisation*

Extracted RNA samples were amplified with T7 RNA polymerase using the Amino Allyl MessageAmp™ aRNA kit (Ambion, Austin, TM) according to the protocol provided by the manufacturer. The quality of each Amino Allyl-aRNA sample was checked on the Agilent 2100 Bioanalyzer. Five micrograms of control and experimental aRNA samples were labelled with Cy3 and Cy5, respectively, mixed and hybridised on an oligonucleotide microarray covering 30,336 human probes (AceGene Human 30K; DNA Chip Research Inc. and Hitachi Software Engineering Co., Yokohama, Japan). The experimental protocol is available at http://www.dna-chip.co.jp/thesis/AceGeneProtocol.pdf. The microarrays were scanned on a ScanArray 4000 (GSI Lumonics, Billerica, MA).

2.4. *Analysis of microarray data*

Signal values were calculated using DNASIS Array Software (Hitachi Software Inc., Tokyo). Following background subtraction, data with low signal intensities were excluded from additional investigation. In each sample, the Cy5/Cy3 ratio values were log-transformed. Then, global equalisation to remove a deviation of the signal intensity between whole Cy3- and Cy5-fluorescence was performed by subtracting the median of all log(Cy5/Cy3) values from each log(Cy5/Cy3) value. Genes with missing values in more than 20% of samples were excluded from further analysis; a total of 16,923 genes out of 30,336 were available for analysis.

2.5. *Gene network analysis*

We further analysed the signature genes of HCC by Ingenuity Pathways Analysis (Ingenuity systems, Mountain View, CA; http://www.ingenuity.com), a web-delivered application that enables biologists to discover, visualise and explore relevant networks significant to their experimental results, such as gene expression array datasets. The application makes use of the Ingenuity Pathways Knowledge Base (IPKB), which contains large amounts of individually modelled relationships between gene objects (e.g., genes, mRNAs and proteins) to dynamically generate significant biological networks and pathways. The submitted genes that are mapped to the corresponding gene objects in the IPKB are called 'focus genes'. The focus genes are used as the starting point for generating biological networks. To start building a network, the Ingenuity software queries the IPKB for interactions between focus genes and all the other genes stored in the IPKB, and then generates a set of networks with a maximum network size of 35 genes. A p value for each network is calculated according to the fit of the user's set of significant genes. This is accomplished by comparing the number of focus genes that participate in a given network relative to the total number of occurrences of those genes in all networks stored in the IPKB. The score of a network is displayed as the negative log of the p value, indicating the probability that a collection of genes equal to or greater than the number in a network could be achieved by chance alone.

2.6. *Selection of candidate genes expressed in HCC*

To identify molecular pathways that may be activated or suppressed in HCC, we used a network knowledge-base approach, Ingenuity Pathway Analysis Software, to analyse genome-wide transcriptional responses in the context of known functional interrelationships amongst proteins, small molecules and phenotypes. The post-normalised genes (16,923 genes) either up- or down-regulated in the microarray data, were uploaded into the IPKB as a tab-delimited text file of GenBank accession numbers. These biological networks comprising 5936 genes are displayed graphically as nodes (genes/gene products) and edges (the biological relationships between the nodes). The nodes are displayed using various shapes that represent the functional class of the gene product. The colour green reflects downregulation of gene expression, and red represents upregulation of gene expression with the significance of that regulation represented by colour intensity. Edges are displayed with various labels that describe the nature of the relationship between the nodes. In this way, simultaneous survey and evaluation of the subnetwork regions enabled us to identify several activated canonical pathways in HCC. We highlighted new molecules linked to the 'hotspot' canonical pathways.

2.7. *Real-time quantitative RT-PCR analysis*

Total RNA (1 μg) was used for reverse transcription, and complementary DNA (cDNA) was generated using the Reverse Transcription System (Promega, Madison, WI) as described previously.[8] Quantification of mRNA expression of the candidate genes listed in Table 2 was performed using a real-time thermal cycler, the LightCycler and detection system (Roche Diagnostics, Mannheim, Germany). For detection of the amplification products, LightCycler-DNA master SYBR green I (Boehringer

Table 2 – Candidate genes and expression ratio of microarray analysis

CDS ID	Gene symbol	Description	Average of Cy5/Cy3
NM_000582	SPP1	Secreted phosphoprotein 1 (osteopontin)	4.69
NM_004484	GPC3	Glypican 3	4.23
NM_004039	ANXA2	Annexin 2	2.86
M38591	S100A10	Cellular ligand of annexin 2	1.97
NM_003380	VIM	Vimentin	1.82

Mannheim, Mannheim, Germany) was used as described previously.[9] Briefly, a 20 μl reaction volume containing 2 μl of cDNA and 0.2 μmol/l of each primer was applied to a glass capillary. The primer sequences, PCR cycle conditions and annealing temperatures are listed in Supplementary Table 1. Quantitative analysis of mRNA was performed using LightCycler analysis software (Roche Diagnostics). The relative expression level of the candidate gene was computed with respect to the internal standard GAPDH mRNA to normalise for variations in the amount of input cDNA. The level of expression of the candidate gene was provided by the ratio, in which each normalised gene value in tissue samples was divided by GAPDH mRNA in the same control reference used in the microarray assay. We compared the ratio of candidate genes between samples randomly selected out of 100 HCC samples.

2.8. *Immunohistochemical staining*

Formalin-fixed, paraffin-embedded samples were cut into 5 μm sections, and these were deparaffinised in xylene and rehydrated through a graded series of ethanol. Immunohistochemical staining was performed using a Vectastain ABC peroxidase kit (Vector Labs, Burlingame, CA) as described previously.[10] Briefly, the sections were treated for antigen retrieval in 0.01 M sodium citrate buffer (pH 6.0) for 40 min at 95 °C, followed by incubation in methanol containing 0.3% hydrogen peroxide at room temperature for 20 min to block endogenous peroxidase. After blocking endogenous biotin, the sections were incubated with normal protein-block serum solution at room temperature for 20 min, to block non-specific staining, and then incubated overnight at 4 °C with anti-ANXA2 (mouse monoclonal IgG, diluted 1:500, Abcam Inc.), anti-S100A10 (mouse monoclonal IgG, diluted 1:400, Swant Inc.) and anti-GPC3 (mouse monoclonal IgG, University of Toronto, Jorge Filmus et al.[11]) as primary antibodies. After washing three times for 5 min in phosphate buffered saline (PBS), sections were incubated with a biotin-conjugated secondary antibody (horse anti-mouse for ANXA2, S100A10 and GPC3) at room temperature for 20 min and finally incubated with peroxidase-conjugated streptavidin at room temperature for 20 min. The peroxidase reaction was then developed with 3,3′-diaminobenzidine tetrachloride (Wako Pure Chemical Industries, Osaka, Japan). Finally, the sections were counterstained with Mayer's haematoxylin. For negative controls, sections were treated the same way except they were incubated with non-immunised rabbit IgG or Tris-buffered saline instead of the primary antibody. Immunohistochemical staining was assessed by two investigators independently, without the knowledge of the corresponding clinicopathological data.

2.9. *Statistical analysis*

Pearson's correlation coefficient, χ^2 test, t-test and Kaplan–Meier plot were analysed using StatView (Version 5.0) software (Abacus Concepts, Berkeley, CA). p values less than 0.05 were considered statistically significant. Hierarchical cluster analysis (HCA) was performed with Euclidean distance coefficient as a similarity coefficient and the unweighted pair group method using arithmetic averages (UPGMA) as the clustering algorithm, using GeneMaths (Version 2.0) software.

3. Results

3.1. *Microarray analysis of gene expression changes in HCC tumours*

Gene expression profiling of primary HCC tumours from 100 patients was examined by DNA microarray. We calculated the mean expression levels of each gene across all HCC samples, and, as a preliminary analysis, identified the top 2% of candidate genes displaying at least a 1.5-fold increase in expression. These highly upregulated genes included α-fetoprotein (AFP; data not shown), a common prognostic marker for HCC (fold change = 1.56), and GPC3, recently identified as a novel tumour marker of HCC (fold change = 4.23; fourth highest upregulation).

3.2. *Identification of biologically relevant networks and potential key genes highly expressed in HCC tumours*

In our global network comprising 5936 genes (Supplementary Fig. 1), we highlighted integrin and Akt/NF-κB signalling as two 'hotspot' pathways that comprised a concentration of upregulated genes. The integrin signalling pathway shown in Fig. 1A (gene subnetworks listed in Supplementary Table 2) was identified as significantly activated in HCC and contained 11 upregulated genes, flagging this pathway as a key regulator in HCC tumourigenesis. This fits with the role of integrin signalling in promoting cell proliferation and cell motility.[12] Furthermore, SPP1 and GPC3 were identified as potential key genes (upregulated with >1.5-fold change), with links to integrin signalling. Similarly, we identified the activation of the Akt/NF-κB pathway shown in Fig. 1B in HCC tumours (gene subnetworks listed in Supplementary Table 3). This signalling pathway contained 12 upregulated genes and plays key roles in many cell processes relevant to tumourigenesis including cell survival and apoptosis.[13] Amongst the genes linked to Akt/NF-κB signalling and that had >1.5-fold change were ANXA2, S100A10 and VIM. Network analysis revealed a link between Akt/NF-κB signalling and both ANXA2 and S100A10 through interactions with β-actin (ACTB) and E-cadherin (CDH1). These candidate genes are listed in Table 2.

3.3. *Quantitative RT-PCR validation of several selected genes*

To validate the microarray data, we performed quantitative RT-PCR for candidate genes in 20 samples randomly selected out of the 100 HCC tissues. We compared gene expression levels generated from quantitative RT-PCR with those from microarray analysis by Pearson's correlation coefficients for each candidate gene and StatView Software (Fig. 2). Each of the five genes analysed showed significant correlation confirming the results obtained by DNA microarray.

3.4. *Immunohistochemical study of glypican 3, Annexin 2 and S100A10 in patient samples*

Of the five genes overexpressed in HCC tumours by RT-PCR, immunohistochemical staining for GPC3 was performed on 10 samples of HCC and surrounding non-cancerous tissues

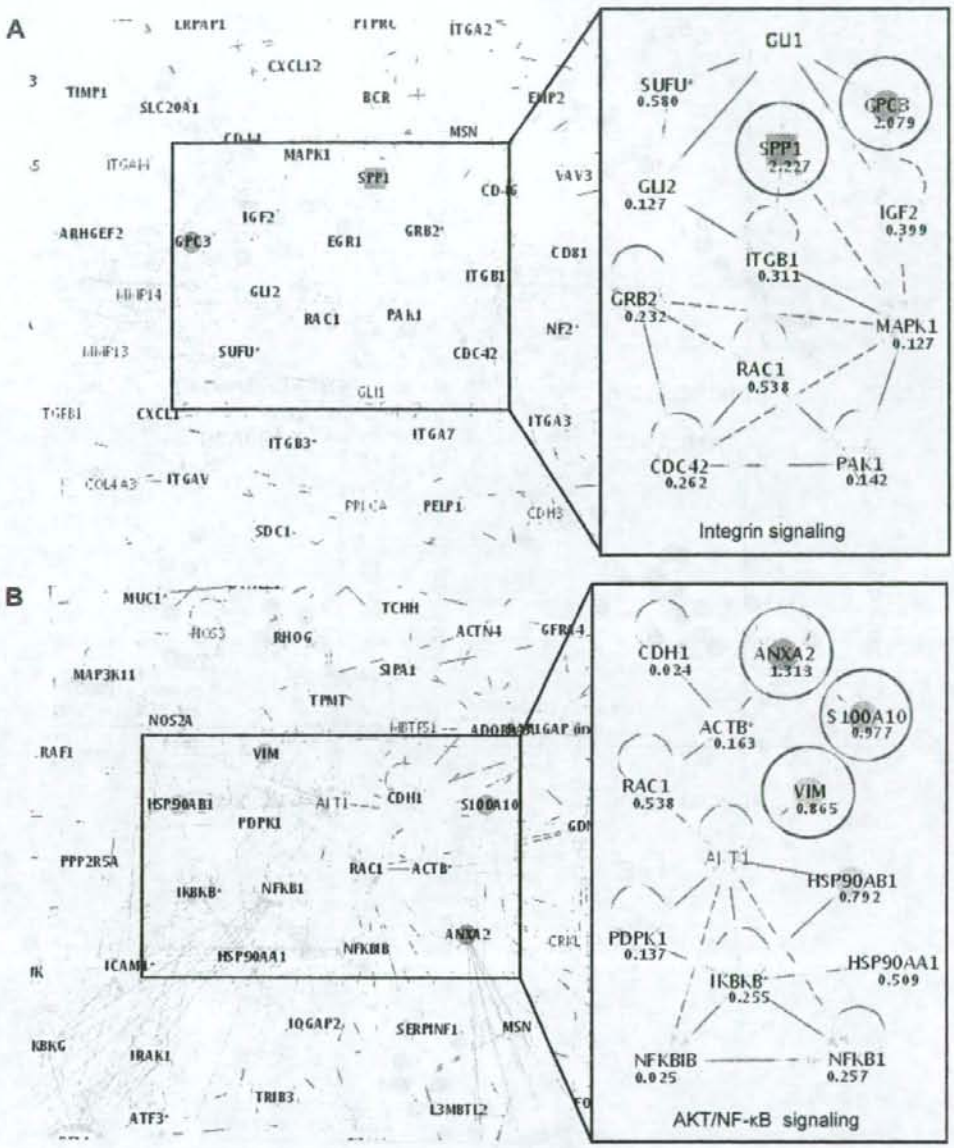

Fig. 1 – (A) The integrated method of DNA microarray and Ingenuity Pathway Analysis produced a network with 'hotspot' regions harbouring concentrations of upregulated genes. These genes included ITGB1 (integrin, beta 1), RAC1 (ras-related C3 botulinum toxin substrate 1), GRB2 (growth factor receptor-bound protein 2), CDC42 (cell division cycle 42), PAK1 (p21/Cdc42/Rac1-activated kinase 1) and MAPK1, which are all associated with integrin signalling. SPP1, GPC3, GLI1, GLI2, SUFU (suppressor of fused homolog) and IGF2 are also linked to this pathway. The circled genes, SPP1 and GPC3, were selected as candidate genes. The numerical value of each gene represents the median of all log(Cy5/Cy3) values. (B) The integrative method showed a second network including a 'hotspot' region. This region contained AKT1 (v-akt murine thymoma viral oncogene homolog 1), PDPK1 (3-phosphoinositide-dependent protein kinase-1), NFKBIB (nuclear factor of kappa light polypeptide gene enhancer in B-cells inhibitor, beta), NFKB1 (nuclear factor of kappa light polypeptide gene enhancer in B-cells 1), IKBKB (inhibitor of kappa light polypeptide gene enhancer in B-cells, kinase beta), HSP90AA1 (heat shock protein 90 kDa alpha, class A member 1) and HSP90AB1 (heat shock protein 90 kDa alpha, class B member 1), which are all associated with the Akt/NF-κB signalling pathway. ANXA2, S100A10, ACTB, CDH1 and VIM are also linked to this pathway. The circled genes, ANXA2, S100A10 and VIM, were selected as candidate genes. The numerical value of each gene represents the average of all log(Cy5/Cy3) values.

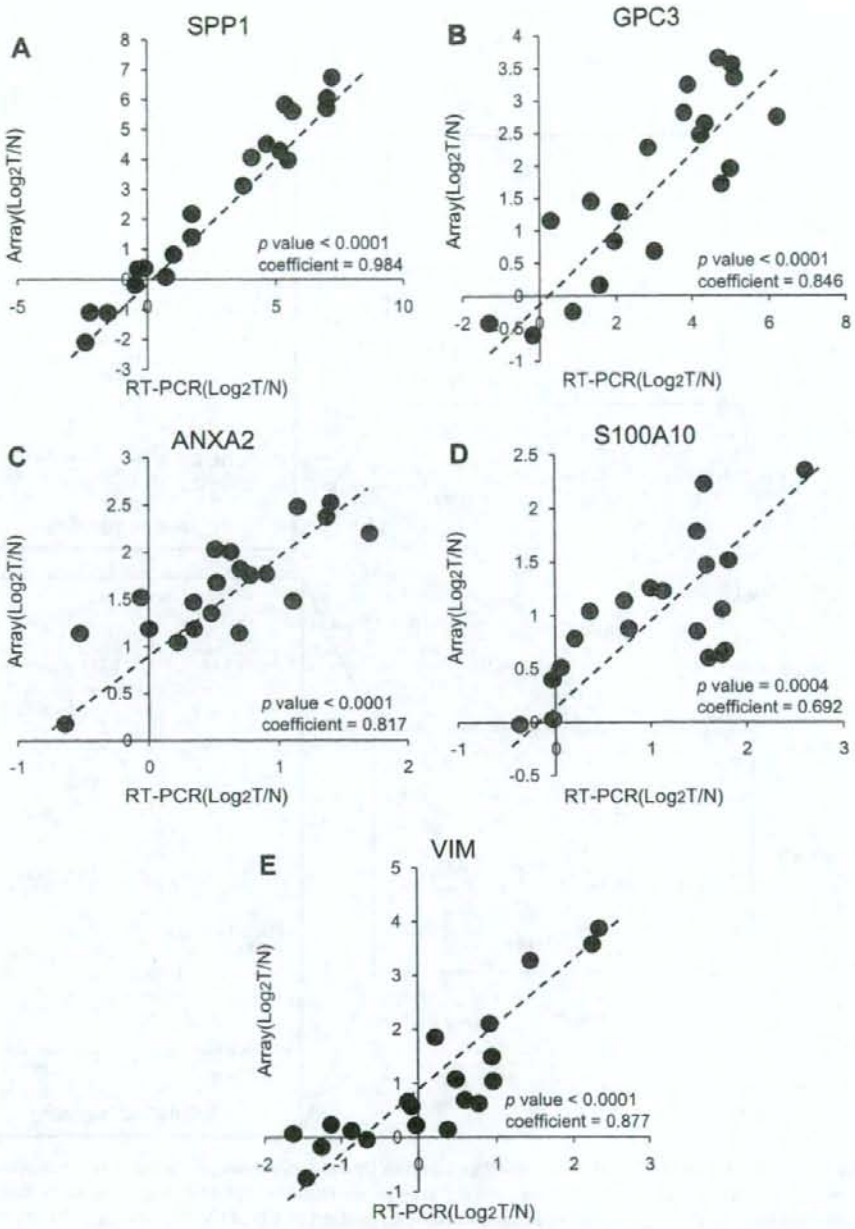

Fig. 2 – Results of quantitative RT-PCR on 20 samples randomly selected from the 100 HCC samples. Individual mRNA levels were normalised to GAPDH and expressed relative to those in a mixture of seven normal livers for SPP1, GPC3, ANXA2, S100A10 and VIM. We compared gene expression levels generated from quantitative RT-PCR with those from microarray analysis and used Pearson's correlation analysis for each candidate gene using StatView Software. (A), (B), (C), (D) and (E) show the correlation of SPP1, GPC3, ANXA2, S100A10 and VIM, respectively.

(Fig. 3A and B). GPC3 expression was observed in 7 of 10 cases of moderately or poorly differentiated HCC. As published previously,[11] staining of GPC3 was observed in a coarsely granular pattern near the cell membrane (2/7) and dispersed evenly in the cytoplasm (5/7). GPC3 expression was undetectable in all non-neoplastic tissues with diffuse hepatitis changes.

Immunohistochemical staining of ANXA2 and S100A10 was then performed on 20 paraffin-embedded samples of HCC and surrounding non-cancerous tissues. The Ca^{2+}-

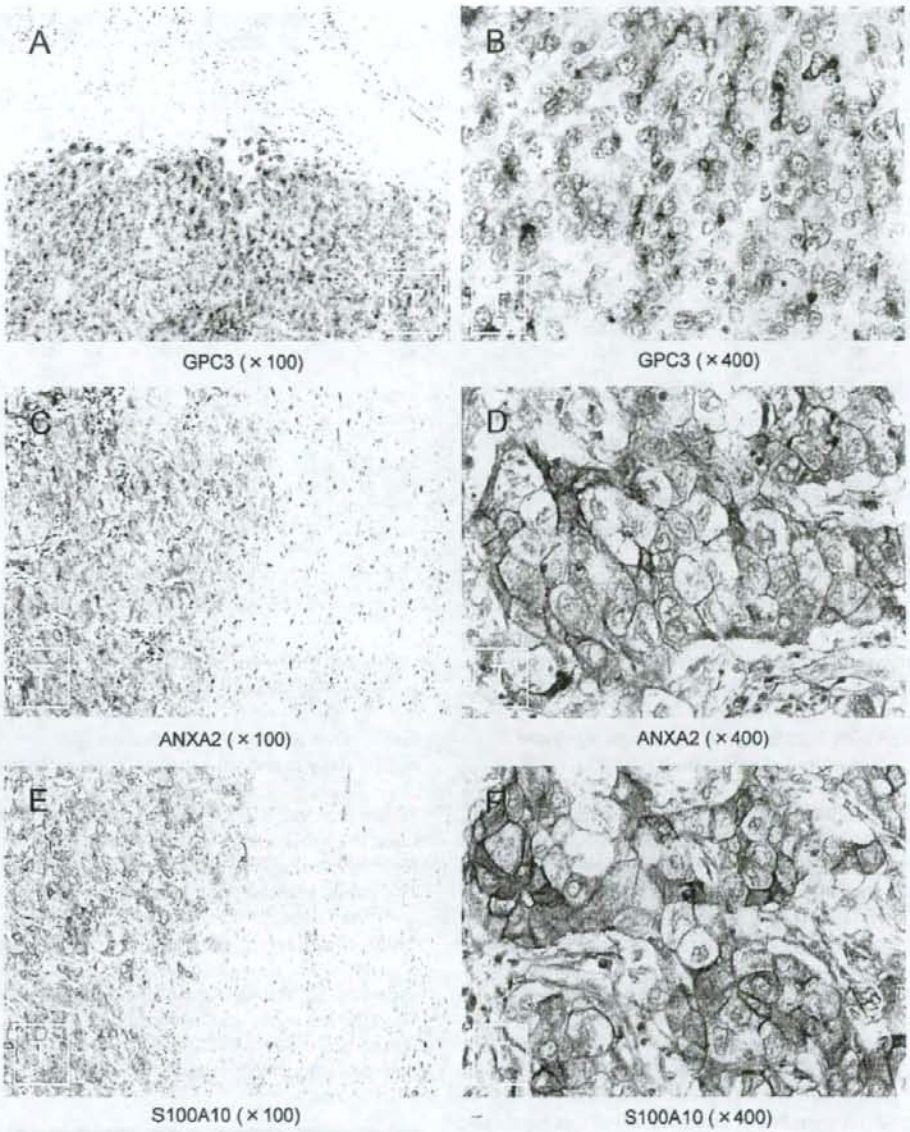

Fig. 3 – (A and B) GPC3 protein expression in human HCC tissue. Brown GPC3 immunostaining is evident in cancer cells. Note the diffuse non-granular staining pattern in the cytoplasm. (C and D) ANXA2 protein expression in human HCC tissue. Note ANXA2 staining in the cell membrane of cancer cells, with slight immunoreactivity in the cytoplasm. (E and F) S100A10 protein expression in human HCC tissues. Note S100A10 staining at the cell membrane of cancer cells. C, D, E and F are from the same tissue sample, and staining for S100A10 overlapped significant with ANXA2 staining. (A, C and E) ×100 magnification. (B, D and F) ×400 magnification. T; tumour region. N; normal liver.

and membrane-binding protein ANXA2 can form a hetero-tetrameric complex with S100A10 and this complex is thought to serve as a bridging or scaffolding function in the membrane underlying cytoskeleton.[14] Previous studies demonstrated both ANXA2 and S100A10 at the plasma membrane in hepatoblastoma HepG2 cell lines,[15] but not in human HCC tissues. Immunohistochemical staining of ANXA2 and S100A10 was stronger at the plasma membrane of the same samples than in the cytoplasm (Fig. 3C–F). The immunoreactivity for ANXA2 was heterogeneous, and cancerous tissues were immunopositive in 16 samples. Endothelial cells were immunopositive for ANXA2 in all samples tested. Similarly, staining of S100A10 was heterogeneous, and cancerous tissues were immunopositive in 17 samples.

Table 3 – Clinicopathological characteristics and results of immunohistochemical staining of ANXA2 and S100A10

Patient	Age	Gender	Hepatitis virus infection	Histological type	Vascular invasion	Annexin2 expression	S100A10 expression
Case 1	71	M	HCV	por	–	++	++
Case 2	66	F	HBV	mod	+	++	++
Case 3	38	M	HBV	mod	+	++	++
Case 4	65	M	HCV	por	+	++	++
Case 5	59	M	HCV	por	–	++	++
Case 6	72	F	HCV	mod	–	+	++
Case 7	71	M	–	por	–	++	+
Case 8	72	M	HBV, HCV	por	–	++	+
Case 9	61	M	–	por	–	++	+
Case 10	78	M	HCV	por	–	++	+
Case 11	49	F	HBV	por	+	++	+
Case 12	72	F	HBV	por	+	+	+
Case 13	68	M	HBV, HCV	mod	–	+	+
Case 14	78	F	HBV, HCV	mod	–	+	+
Case 15	74	M	HBV, HCV	well	–	+	+
Case 16	67	M	–	mod	–	–	+
Case 17	53	M	HBV	mod	+	–	–
Case 18	75	M	HCV	por	–	–	–
Case 19	66	M	HBV, HCV	mod	+	–	–
Case 20	60	M	HCV	por	–	–	–

++, strong immunopositive; +, partial immunopositive; –, immunonegative.

Colocalisation of ANXA2 and S100A10 was observed in 15 samples (Table 3).

3.5. *Correlation between gene expression signature of the two 'hotspot' and clinicopathological features*

Next, to better understand if any of the two 'hotspot' identified by this integrated approach correlates with clinicopathological features, a hierarchical clustering of all 100 HCC samples using the upregulated genes included in the 'hotspot' was performed. Fig. 4A shows the gene expression profiles using the 11 genes upregulated in the 'hotspot 1 (integrin signalling)'. Examination of this result allowed identification of three subgroups; 'relatively high-activated group ($n = 39$), defined as Group A1', 'intermediate-activated group ($n = 45$), defined as Group A2', and 'relatively low-activated group ($n = 16$), defined as Group A3'. Likewise, Fig. 4B shows the gene expression profiles using the 12 genes upregulated in the 'hotspot 2 (Akt/NF-κB signalling)'. Examination of this result also identified two subgroups; 'relatively high-activated group ($n = 17$), defined as Group B1' and 'relatively low-activated group ($n = 83$), defined as Group B2'. Having identified the two distinctive subgroups; 'relatively high-activated group' and 'relatively low-activated group' in each of the two 'hotspots', we examined the association between the activation of 'hotspot' and clinicopathological data (Table 4A and B). In the integrin signalling, the activated profile was significantly associated with intrahepatic metastasis ($p = 0.012$), tumour size ($p = 0.023$) and Edmonson grading ($p < 0.001$). On the other hand, in the Akt/NF-κB signalling, the activated profile was significantly associated with Edmonson grading ($p = 0.004$). Kaplan–Meier plot showed a significant difference in the probability of disease-free survival ($p = 0.037$) and overall survival ($p = 0.045$) between 'Group A1' and 'Group A3' in the integrin signalling (Fig. 4C and D). In the Akt/NF-κB signalling, a significant difference was observed in disease-free survival ($p = 0.045$, Fig. 4E and F).

3.6. *Overview of the distribution of differentially expressed genes on human chromosome*

To compare our microarray data with chromosomal aberrations in HCC, we also investigated the chromosomal region in which the differentially expressed genes were harboured. The public source for annotating the location of each gene was the National Center for Biotechnology Information (NCBI). This investigation revealed that the regions of high density of 100 upregulated genes tended to be at chromosomes 1q, 6p and 8q (Fig. 5A), whilst those of 100 downregulated genes were at chromosomes 4q and 16q (Fig. 5B). Furthermore, SPP1, GPC3, ANXA2 and S100A10, identified as key molecules, were separately located at chromosomes 4q, Xq, 15q and 1q.

4. Discussion

In the post-genomic period, DNA microarray technology is used to monitor disease progress and to individualise treatment regimens. However, extracting new biological insights from high-throughput genomic studies of cancer progression poses a challenge due to difficulties in recognising and evaluating relevant biological processes from vast quantities of experimental data. Although other high-throughput technologies in protein expression (proteomics) and low-molecular weight metabolite expression (metabolomics) have made remarkable progress, no comprehensive analytical techniques exist that can measure more than 500,000 protein forms and 100,000–1,000,000 metabolites quantitatively.[16] Generating biological networks from comprehensive gene expression profiles manually in a visual manner could be used to navigate

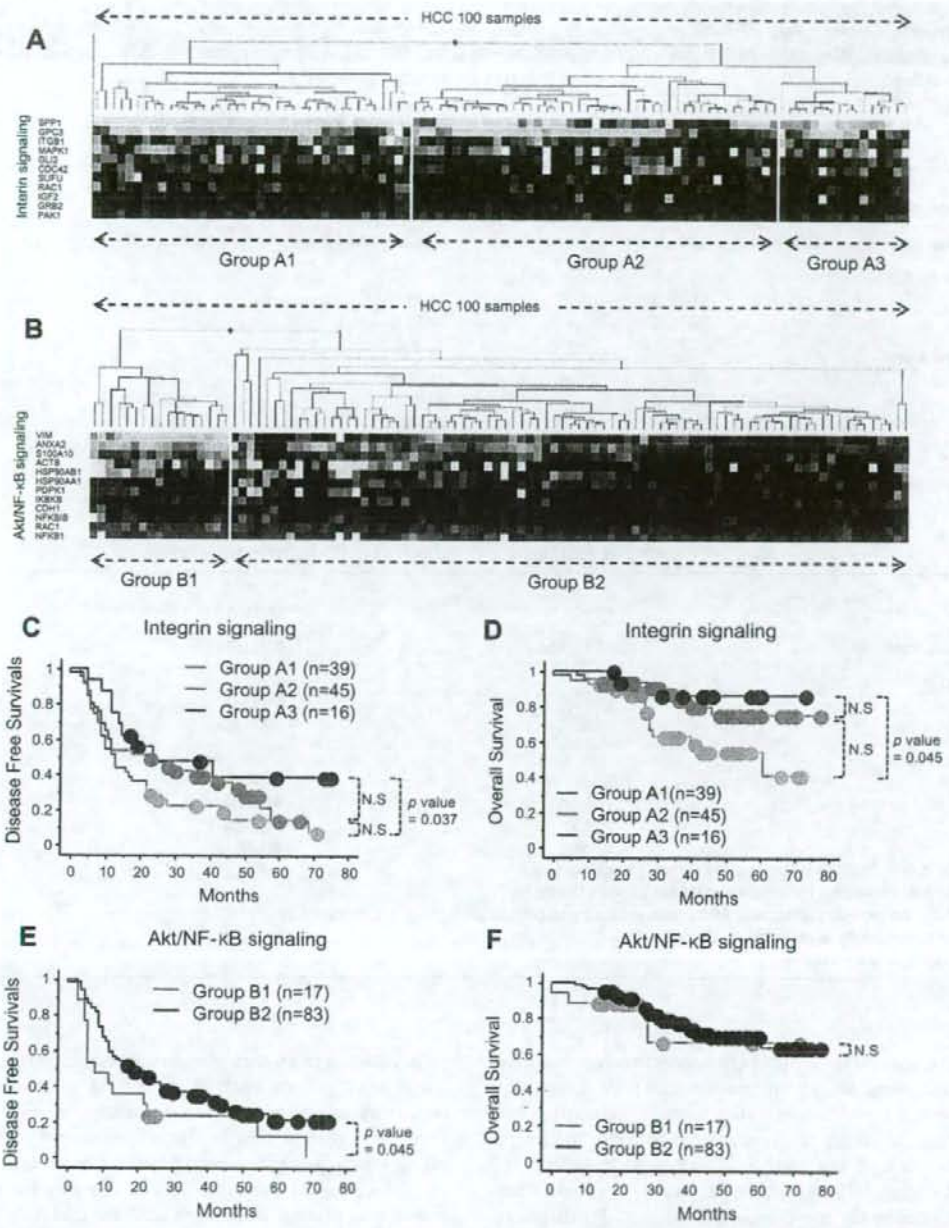

Fig. 4 – (A) Hierarchical clustering analysis of all 100 HCC samples using the 11 upregulated genes included in the 'hotspot 1 (integrin signalling)'. Red and green indicate relative high- and low-expression, respectively. Based on the similarities of their gene expression profiles, samples were grouped in 'relatively high-activated group ($n = 39$), defined as Group A1', 'intermediate-activated group ($n = 45$), defined as Group A2', and 'relatively low-activated group ($n = 16$), defined as Group A3'. (B) A hierarchical clustering analysis of all 100 HCC samples using the 12 upregulated genes included in the 'hotspot 2 (Akt/NF-κB signalling)'. Based on the similarities of their gene expression profiles, samples were grouped in 'relatively high-activated group ($n = 17$), defined as Group B1' and 'relatively low-activated group ($n = 83$), defined as Group B2'. (C and D) Disease-free survival and overall survival of each of the activated groups in the 'hotspot 1 (integrin signalling)' (Kaplan–Meier plot). The log-rank p value is shown. NS, not significant. (E and F) Disease-free survival and overall survival of each of the activated groups in the 'hotspot 2 (Akt/NF-κB signalling)' (Kaplan–Meier plot). The log-rank p value is shown. NS, not significant.

Table 4 – Clinical and pathological characteristics of the high-activated and low-activated groups in each of integrin signalling and AKT/NF-κB signalling

Characteristics	Integrin signalling ('Hotspot' 1)			p value
	Group A1 (n = 39)	Group A2 (n = 45)	Group A3 (n = 16)	
	No. of patients (%)	No. of patients (%)	No. of patients(%)	
A				
Intrahepatic metastasis	12(30.8)	(10(22.2))	0(0)	0.012
Tumour size (cm)	4.79 ± 3.12	(3.49 ± 1.75)	2.91 ± 1.22	0.023
Edmonson grading				
1–2	11(28.2)	22(48.9)	10(62.5)	<0.001
3–4	28(71.8)	23(51.1)	6(37.5)	
Pathological stage				
I	5(12.8)	15(33.3)	3(18.7)	0.642
II	22(56.4)	20(44.4)	10(62.5)	
III	9(23.1)	8(17.8)	3(18.7)	
IVA	3(7.7)	2(4.5)	0	

Characteristics	Akt/NF-κB signalling ('Hotspot' 2)		p value
	Group B1 (n = 17)	Group B2 (n = 83)	
	No. of patients (%)	No. of patients (%)	
B			
Intrahepatic metastasis	4(23.5)	18(21.7)	0.867
Tumour size (cm)	4.55 ± 2.58	3.88 ± 2.81	0.226
Edmonson grading			
1–2	2(11.7)	41(49.4)	0.004
3–4	15(88.3)	42(50.6)	
Pathological stage			
I	1(5.9)	22(26.5)	0.333
II	11(64.7)	41(49.4)	
III	4(23.5)	16(19.3)	
IVA	1(5.9)	4(4.8)	

p values of A are obtained by comparing Group A1 with Group A3.
p values of B are obtained by comparing Group B1 with Group B2.
p values for intrahepatic metastasis, Edmonson grading and pathological stage are obtained by χ^2 test.
p value for tumour size is obtained by t test.
Tumour size is mean ± SD.

through and unravel the complex networks involved in cancer progression. Here, we combined genome-wide expression analysis with a new bioinformatics method, Ingenuity Pathway Analysis, to clarify the relationship between the microarray datasets and the canonical pathways based on the published literature and identify functional networks, 'hotspot', responsible for the progression of HCC. Furthermore, we discovered several molecules commonly upregulated in HCC as potential key players in the neoplastic process.

This combined approach revealed that several distinct regions with upregulated genes were concentrated. These concentrations of activated genes included several genes involved in the WNT signalling pathway, which has been the subject of intense research in recent years. In addition, we highlighted integrin and Akt/NF-κB as two 'hotspot' signalling pathways, and propose that these signalling pathways are crucial for the core biological functions in HCC progression and potential intervention, such as cell proliferation, cell survival and apoptosis.[17]

In addition to studies of gene expression at the transcriptional level, protein analysis is vital for understanding the regulatory processes in living organisms, because emerging evidence suggests that mRNA expression patterns themselves are necessary but insufficient for quantitative description of biological systems. So far, comparative studies of mRNA and protein abundance indicate that only 20–28% of the total variation of protein abundance can be attributed to mRNA abundance alone.[18] The limiting factors were explained partly by translational processes (microRNAs repress the translation of mRNAs into proteins) and post-translational modification (such as phosphorylation, methylation, acetylation, glycosylation and ubiquitination). In fact, this was the basis for investigating the expression levels of proteins encoded by highly upregulated genes related to key signalling pathways in hepatocarcinogenesis.

Using our analysis protocol, integrin pathway-associated molecules, SPP1 and GPC3, were first identified as key for cell proliferation in HCC. HCC generally spreads throughout the

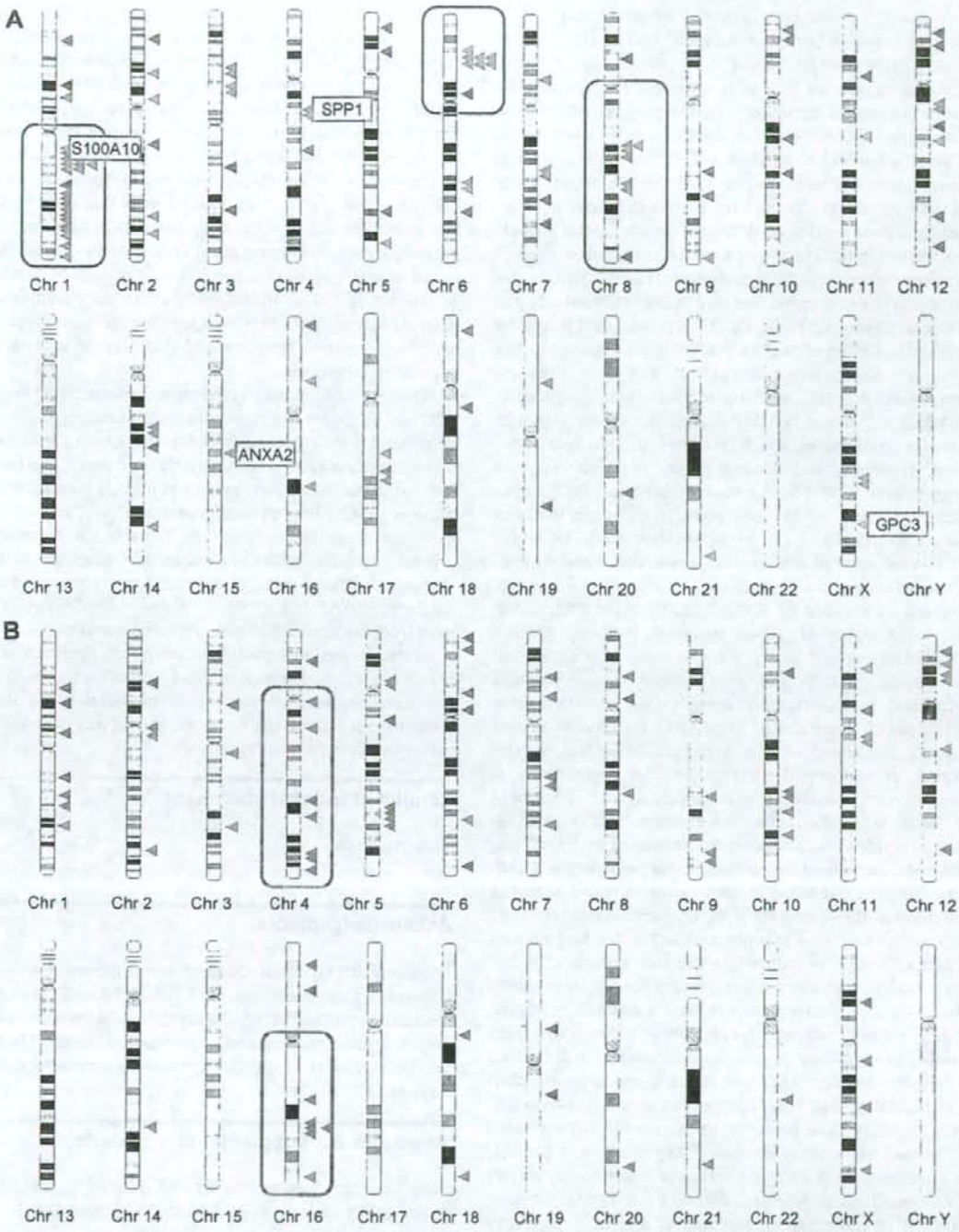

Fig. 5 – Location of 100 upregulated genes (A) and 100 downregulated genes (B) on human chromosomes. Upregulated genes are represented as red arrows, and downregulated genes are represented as blue arrows. Red-coloured circles (chromosomes 1q, 6p and 8q) represent regions with relative concentration of upregulated genes, whilst blue coloured circles (chromosomes 4q and 16q) represent regions with relative concentration of down-regulated genes. ANXA2, S100A10, SPP1 and GPC3 are located at chromosomes 15q21-22, 1q22, 4q21-25 and Xq26.1, respectively.

liver via the portal vein system even in advanced stages, and portal vein invasion is the most crucial histological feature associated with poor prognosis.[3] SPP1 protein expression is upregulated in primary HCC with accompanying metastasis, and SPP1 expression correlates with the invasiveness of HCC cells in tissue culture.[19] Based on network analysis, we speculated that the binding of integrins to SPP1[20] might be related to the progression and metastasis of HCC. GPC3, a heparan sulphate proteoglycan anchored to the plasma membrane, is also a good candidate marker of HCC. It is an oncofoetal protein overexpressed in HCC at both the mRNA and protein levels.[11] We also confirmed that GPC3 was overexpressed in HCC by the immunostaining of paraffin sections. In the activated integrin pathway, GPC3 interacts with IGF-2,[21] a protein that increases the phosphorylation of MAPK1.[22] GPC3 is also related to the zinc-finger transcription factors, GLI1 and GLI2, that are known players in WNT signalling and Sonic hedgehog signalling pathways.[23] Recently, WNT signalling was implicated in hepatocyte proliferation, which could be crucial in liver development, regeneration following partial hepatectomy, and pathogenesis of HCC.[24] In this context, SPP1 and GPC3 might participate in the activation of integrin signalling in HCC and based on the results of clustering analysis, might be implicated as mediators of intrahepatic metastasis, histopathological malignancy or poor prognosis.

Second, we focused on ANXA2, S100A10 and VIM, which were related to the Akt/NF-κB signalling pathway. ANXA2, also called calpactin I heavy chain, is a member of the annexin family of Ca^{2+}- and phospholipid-binding proteins and forms a heterotetrameric complex with S100A10, also called calpactin I light chain.[25] The ANXA2-S100A10 complex has been implicated in the structural organisation and dynamics of endosomal membranes, the organisation of cholesterol-rich membrane microdomains, and connecting lipid rafts with the actin cytoskeleton.[25] The ANXA2-S100A10 complex was also recently associated with recycling endosomes, and might be involved in the recycling of E-cadherin during the formation of the E-cadherin-based adherens junctions via the modulation of the actin cytoskeleton.[26] Moreover, ANXA2 was identified as a Rac binding partner and Rac activation is induced by the interactions of E-cadherin in the formation of adherens junctions.[27] In this way, cadherin–cadherin interactions initiate a cascade of signalling events that result in increased cadherin/Akt association, activation of Akt/NF-κB signalling, and increased cell survival and tumour growth.[27] Akt1 was found to associate structurally with VIM (a structural component of intermediate filaments),[28] which has been found in poorly differentiated HCC as well as hepatoblastomas.[29] Therefore, it is possible that binding of Akt1 and VIM activates downstream players (NF-κB signalling) as well as increasing the intrinsic activity of Akt1. This molecular understanding of HCC progression in Akt/NF-κB signalling was not so different from our result of correlations between clinicopathological features and gene expression profiles. It seems that the higher-activated group in Akt/NF-κB signalling has lower histopathological differentiation.

Currently, the array-based CGH approach is used to study chromosomal aberrations in human cancers. A previously reported meta-analysis[30] showed that the most common chromosomal arms containing gains were 1q, 6p and 8q, whereas the most common losses were found in chromosomes 4q, 8p and 16q. Comparing our expression data with the meta-analysis result of array-based CGH in HCC,[30] we found that our gene expression data surprisingly matched the chromosomal aberrations. The comprehensive analysis of 100 HCC samples using human 30 K DNA microarray revealed a potential association between the global copy number and expression. It is also noteworthy that our identified key molecules that operate synergistically in hepatocarcinogenesis are located at separate chromosomes, so chromosomal aberrations cannot prove a relationship of candidate genes such as ANXA2 and S100A10. Therefore, our integrative network approach can provide a significant clue to the discovery of novel genetic combinations that may be important for hepatocarcinogenesis.

Here, we highlighted the 'hotspot' canonical pathways in HCC and improved our molecular understanding of HCC progression. It is widely recognised that there are distinct molecular subtypes of HCC in the transcriptome space, and current interest of the community spread to include identification of subtype-specific aberration of genes/pathway. This functional genomics study could contribute towards the detection of several signalling pathways commonly activated in HCC. Moreover, we succeeded in detecting two potential disease markers, ANXA2 and S100A10, whose colocalisation in human HCC tissues has not been reported previously.

In conclusion, we reported an integrative approach of genome-wide microarray analysis and network analysis in HCC. This novel approach allows the extraction of deeper biological insight from microarray data and identifying potential key molecules in hepatocarcinogenesis.

Conflict of interest statement

None declared.

Acknowledgements

We thank EIJI MIYOSHI, Department of Biochemistry, Osaka University Medical School, and JORGE FILMUS, Division of Molecular and Cell Biology, Sunnybrook and Women's College Health Sciences Centre and Department of Medical Biophysics, University of Toronto, for providing a monoclonal antibody of GPC3.

Appendix A. Supplementary material

Supplementary data associated with this article can be found, in the online version, at doi:10.1016/j.ejca.2008.02.019.

REFERENCES

1. Thomas MB, Abbruzzese JL. Opportunities for targeted therapies in hepatocellular carcinoma. *J Clin Oncol* 2005;23:8093–108.

2. Jemal A, Murray T, Ward E, Samuels A, Tiwari RC, Ghafoor A. Cancer statistics, 2005. *CA Cancer J Clin* 2005;**55**:10–30.
3. Pan HW, Ou YH, Peng SY, Liu SH, Lai PL, Lee PH. Overexpression of osteopontin is associated with intrahepatic metastasis, early recurrence, and poorer prognosis of surgically resected hepatocellular carcinoma. *Cancer* 2003;**98**:119–27.
4. Tsou AP, Wu KM, Tsen TY, Chi CW, Chiu JH, Lui WY. Parallel hybridization analysis of multiple protein kinase genes: identification of gene expression patterns characteristic of human hepatocellular carcinoma. *Genomics* 1998;**50**:331–40.
5. Schadt EE, Monks SA, Drake TA, Lusis AJ, Che N, Colinayo V. Genetics of gene expression surveyed in maize, mouse and man. *Nature* 2003;**422**:297–302.
6. Brem RB, Yvert G, Clinton R, Kruglyak L. Genetic dissection of transcriptional regulation in budding yeast. *Science* 2002;**296**:752–5.
7. Thorgeirsson SS, Grisham JW. Molecular pathogenesis of human hepatocellular carcinoma. *Nat Genet* 2002;**31**:339–46.
8. Slaton JW, Perrotte P, Inoue K, Dinney CP, Fidler IJ. Interferon-alpha-mediated down-regulation of angiogenesis-related genes and therapy of bladder cancer are dependent on optimization of biological dose and schedule. *Clin Cancer Res* 1999;**5**:2726–34.
9. Yamamoto T, Nagano H, Sakon M, Wada H, Eguchi H, Kondo M. Partial contribution of tumour necrosis factor-related apoptosis-inducing ligand (TRAIL)/TRAIL receptor pathway to antitumor effects of interferon-alpha/5-fluorouracil against hepatocellular carcinoma. *Clin Cancer Res* 2004;**10**:7884–95.
10. Kondo M, Yamamoto H, Nagano H, Okami J, Ito Y, Shimizu J. Increased expression of COX-2 in nontumor liver tissue is associated with shorter disease-free survival in patients with hepatocellular carcinoma. *Clin Cancer Res* 1999;**5**:4005–12.
11. Capurro M, Wanless IR, Sherman M, Deboer G, Shi W, Miyoshi E. Glypican-3: a novel serum and histochemical marker for hepatocellular carcinoma. *Gastroenterology* 2003;**125**:89–97.
12. Zhang H, Ozaki I, Mizuta T, Yoshimura T, Matsuhashi S, Hisatomi A. Mechanism of beta 1-integrin-mediated hepatoma cell growth involves p27 and S-phase kinase-associated protein 2. *Hepatology* 2003;**38**:305–13.
13. Mottet D, Dumont V, Deccache Y, Demazy C, Ninane N, Raes M. Regulation of hypoxia-inducible factor-1alpha protein level during hypoxic conditions by the phosphatidylinositol 3-kinase/Akt/glycogen synthase kinase 3beta pathway in HepG2 cells. *J Biol Chem* 2003;**278**:31277–85.
14. Puisieux A, Ji J, Ozturk M. Annexin II up-regulates cellular levels of p11 protein by a post-translational mechanisms. *Biochem J* 1996;**313**:51–5.
15. Zobiack N, Gerke V, Rescher U. Complex formation and submembranous localization of annexin 2 and S100A10 in live HepG2 cells. *FEBS Lett* 2001;**500**:137–40.
16. Hollywood K, Brison DR, Goodacre R. Metabolomics: current technologies and future trends. *Proteomics* 2006;**6**:4716–23.
17. Cantley LC. The phosphoinositide 3-kinase pathway. *Science* 2002;**296**:1655–7.
18. Mootha VK, Bunkenborg J, Olsen JV, et al. Integrated analysis of protein composition, tissue diversity, and gene regulation in mouse mitochondria. *Cell* 2003;**115**:629–40.
19. Ye QH, Qin LX, Forgues M, He P, Kim JW, Peng AC. Predicting hepatitis B virus-positive metastatic hepatocellular carcinomas using gene expression profiling and supervised machine learning. *Nat Med* 2003;**9**:416–23.
20. Hu DD, Lin EC, Kovach NL, Hoyer JR, Smith JW. A biochemical characterization of the binding of osteopontin to integrins alpha v beta 1 and alpha v beta 5. *J Biol Chem* 1995;**270**:26232–8.
21. Song HH, Shi W, Filmus J. OCI-5/rat glypican-3 binds to fibroblast growth factor-2 but not to insulin-like growth factor-2. *J Biol Chem* 1997;**272**:7574–7.
22. Moorehead RA, Sanchez OH, Baldwin RM, Khokha R. Transgenic overexpression of IGF-II induces spontaneous lung tumors: a model for human lung adenocarcinoma. *Oncogene* 2003;**22**:853–7.
23. Regl G, Kasper M, Schnidar H, Eichberger T, Neill GW, Ikram MS. The zinc-finger transcription factor GLI2 antagonizes contact inhibition and differentiation of human epidermal cells. *Oncogene* 2004;**23**:1263–74.
24. Apte U, Zeng G, Muller P, Tan X, Micsenyi A, Cieply B. Activation of Wnt/beta-catenin pathway during hepatocyte growth factor-induced hepatomegaly in mice. *Hepatology* 2006;**44**:992–1002.
25. Gerke V, Moss SE. Annexins: from structure to function. *Physiol Rev* 2002;**82**:331–71.
26. Yamada A, Irie K, Hirota T, Ooshio T, Fukuhara A, Takai Y. Involvement of the annexin II-S100A10 complex in the formation of E-cadherin-based adherens junctions in Madin–Darby canine kidney cells. *J Biol Chem* 2005;**280**:6016–27.
27. Kovacs EM, Ali RG, McCormack AJ, Yap AS. E-cadherin homophilic ligation directly signals through Rac and phosphatidylinositol 3-kinase to regulate adhesive contacts. *J Biol Chem* 2002;**277**:6708–18.
28. Siu MK, Wong CH, Lee WM, Cheng CY. Sertoli-germ cell anchoring junction dynamics in the testis are regulated by an interplay of lipid and protein kinases. *J Biol Chem* 2005;**280**:25029–47.
29. Abenoza P, Manivel JC, Wick MR, Hagen K, Dehner LP. Hepatoblastoma: an immunohistochemical and ultrastructural study. *Hum Pathol* 1987;**18**:1025–35.
30. Moinzadeh P, Breuhahn K, Stutzer H, Schirmacher P. Chromosome alterations in human hepatocellular carcinomas correlate with aetiology and histological grade–results of an explorative CGH meta-analysis. *Br J Cancer* 2005;**92**:935–41.